Miner Petrol (2017) 111:833–842
DOI 10.1007/s00710-017-0495-1

ORIGINAL PAPER

Alumovesuvianite, $Ca_{19}Al(Al,Mg)_{12}Si_{18}O_{69}(OH)_9$, a new vesuvianite-group member from the Jeffrey mine, asbestos, Estrie region, Québec, Canada

Taras L. Panikorovskii[1] · **Nikita V. Chukanov**[2] · **Sergey M. Aksenov**[3,4] · **Anton S. Mazur**[5] · **Evgenia Yu Avdontseva**[1] · **Vladimir V. Shilovskikh**[6] · **Sergey V. Krivovichev**[1]

Received: 1 December 2016 / Accepted: 23 January 2017 / Published online: 4 February 2017

Abstract Alumovesuvianite (IMA 2016–014), ideally $Ca_{19}Al(Al,Mg)_{12}Si_{18}O_{69}(OH)_9$, is a new vesuvianite-group member found in the rodingite zone at the contact of a gabbroid rock with host serpentinite in the abandoned Jeffrey mine, Asbestos, Estrie Region, Québec, Canada. It occurs as prismatic tetragonal crystals up to $4 \times 4 \times 6$ mm^3 in size encrusting walls of cavities in a granular diopside. Associated minerals are diopside, grossular and prehnite. Single crystals of alumovesuvianite are transparent colorless or light pink with a vitreous lustre. The dominant crystal forms are {100}, {110}, {210}, {111}, {101} and {001}. The Mohs hardness is 6.5. The specific gravitiy is D_{meas} = 3.31(1) g/cm^3 and D_{calc} = 3.36 g/cm^3, respectively. The mineral is optically uniaxial (−), $\omega = 1.725(2)$, $\varepsilon = 1.722(2)$. The chemical composition, determined by SEM–WDS (wavelength-dispersive spectroscopy on a scanning electron microscope; all oxides except H_2O) and TG (thermogravimety; H_2O) analysis, is: SiO_2 37.1 wt%, Al_2O_3 18.8 wt%, CaO 36.6 wt%, MgO 2.48 wt%, Mn_2O_3 0.67 wt%, Fe_2O_3 0.22 wt%, H_2O 2.61 wt%, total 98.5 wt%. The empirical formula based on 19 Ca atoms per formula unit and taking into account the MAS–NMR (magic-angle spinning nuclear magnetic resonance) data, is: $Ca_{19.00}(Al_{0.92}Fe^{3+}_{0.08})_{\Sigma 1.00}(Al_{9.83}Mg_{1.80}Mn^{3+}_{0.25})_{\Sigma 11.88}Si_{17.98\text{-}}O69.16(OH)_{8.44}$. The most intense IR absorption bands lie in the ranges 412–609, 897–1024, and 3051–3671 cm^{-1}. The eight strongest lines of the powder X-ray diffraction pattern are (*I*–*d*(Å)–*hkl*): 22–2.96–004, 100–2.761–432, 61–2.612–224, 25–2.593–600, 20–1.7658–831, 20–1.6672–734, 21–1.6247–912, and 22–1.3443–880. Alumovesuvianite is tetragonal, space group $P4/n$, unit-cell parameters refined from the powder data are a = 15.5603(5) Å, c = 11.8467(4) Å, V = 2868.3(4) Å^3, Z = 2. The crystal structure has been refined to R_1 = 0.036 for 3098 unique observed reflections with $|F_o| \geq 4\sigma_F$. The structure refinement provides the $<Y1A\text{–}O>$ bond length of 1.916 Å and the scattering factor for the $Y1$ site of 16 e^-, which is in good agreement with the total occupancy of this site as $(Al_{0.73}Mn^{3+}_{0.20}Fe^{3+}_{0.07})_{\Sigma 1.00}$ and is confirmed by the ^{27}Al MAS NMR data. Alumovesuvianite is a new member of the vesuvianite group with Al^{3+} as a dominant cation in the $Y1$ site. The name alumovesuvianite is given to highlight the species-defining role of Al.

Keywords Alumovesuvianite · New mineral · Vesuvianite group · Structure relaxation · Cation ordering · Jeffrey mine · Asbestos · Canada

---

Editorial handling: L. Bindi

Electronic supplementary material The online version of this article (doi:10.1007/s00710-017-0495-1) contains supplementary material, which is available to authorized users.

✉ Taras L. Panikorovskii
taras.panikorovsky@spbu.ru

[1] Department of Crystallography, St. Petersburg State University, University Emb. 7/9, St. Petersburg 199034, Russia

[2] Institute of Problems of Chemical Physics, Russian Academy of Sciences, Chernogolovka 142432, Russia

[3] Institute of Crystallography, Russian Academy of Sciences, Leninskiy Prospekt 59, Moscow 117333, Russia

[4] Faculty of Geology, Moscow State University, Vorobievy Gory, Moscow 119991, Russia

[5] Center for Magnetic Resonance, St. Petersburg State University, University Av. 26, St. Petersburg 198504, Russia

[6] Institute of Chemistry, St. Petersburg State University, University Av. 26, St. Petersburg 198504, Russia

Fig. 1 Aggregate of alumovesuvianite crystals

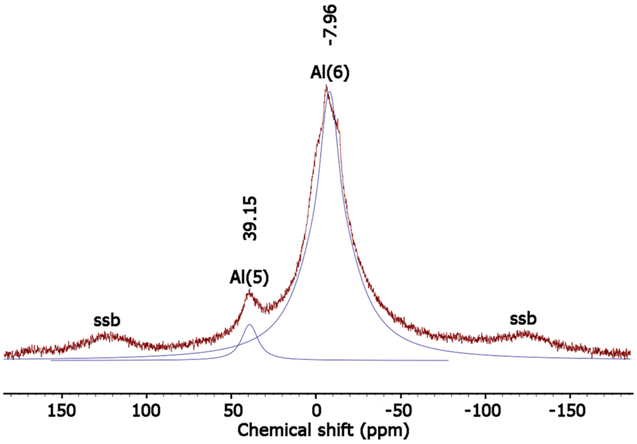

Fig. 3 ^{27}Al MAS NMR spectrum of alumovesuvianite. Spinning sidebands are marked "ssb"

Introduction

Members of the vesuvianite group attract considerable attention of mineralogists, petrologists and crystallographers for a long time, because of the high complexity of their crystal structures (Krivovichev 2013), wide chemical variations (Groat et al. 1992), and structure relaxation mechanisms (Armbruster and Gnos 2000b). Owing to their domain structure and cation ordering, they can be considered as indicators of formation conditions for a wide range of geological settings (Gnos and Armbruster 2006). During the last twenty years, six new minerals of the vesuvianite group were approved by the IMA Commission on New Minerals, Nomenclature and Classification (IMA CNMNC).

The general formula of vesuvianite-group minerals can be written as follows ($Z = 2$): $X_{16}X1_2X4Y1Y2_4Y3_8T_{0–5}[(ZO_4)_{10-x}(H_4O_4)_x](Z_2O_7)_4(W)_{10–12}$, where $x < 3$; X are seven- to nine-coordinated sites with Ca as a major and Na, K, Fe^{2+}, and *REE* as subordinate components; $X1$ and $X4$ are in a square antiprism coordination (Ca, Na), $Y1$ is in a square pyramidal coordination and can be occupied by Fe^{3+}, Mg, Al, Fe^{2+}, or Cu^{2+}; $Y2$ and $Y3$ have octahedral coordinations (Al, Mg, Zn, Fe^{2+}, Fe^{3+}, Mn^{2+}, Mn^{3+}, Ti, Cr); T (B, Fe, Al) is the additional site with a triangular and/or tetrahedral coordination, whereas ZO_4 (SiO_4, H_4O_4) and Z_2O_7 are ortho- and ditorthosilicate groups, respectively, and W = OH or O, F, Cl (Machatschki 1932; Coda et al. 1970; Groat et al. 1992; Dyrek et al. 1992; Galuskin et al. 2003, 2007; Galuskin et al. 2005; Aksenov et al. 2016; Panikorovskii et al. 2016a, 2016b, 2016c, 2016d, 2016e).

The crystal structure of vesuvianite-group minerals has a modular character. One-dimensional grossular-type modules (Allen and Burnham 1992) running along the fourfold axis are connected by the Si_2O_7 groups to form a heteropolyhedral framework with the channels ('rods') occupied by half-populated (in the $P4/nnc$ structure model) $Y1$A,B and $X4$A,B sites (Fig. 7). Within the channels cation sites are ordered following the sequence $Y1$A–$X4$A–$X4$B–$Y1$B showing distances shorter than 1.3, 1.3 and 2.5 Å between the $Y1$A–$X4$A, $Y1$A–$X4$A and $X4$A–$X4$B sites, respectively. Cation ordering at the $Y1$A,B and $X4$A,B sites results in different ordering schemes and, as a result, in different space groups (Giuseppetti and Mazzi

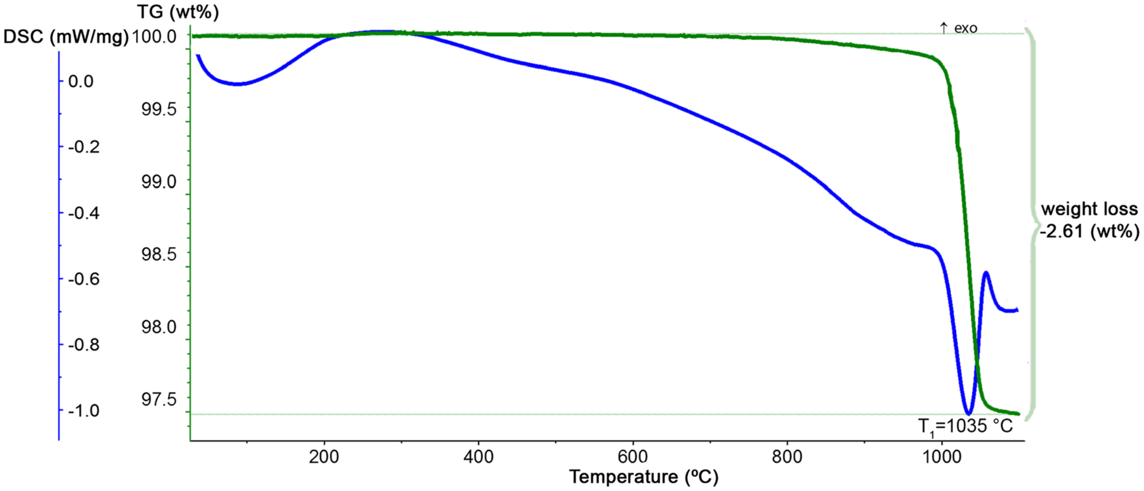

Fig. 2 TGA weight loss (wt%, *green*) and DSC (*blue*) graphs of alumovesuvianite

Fig. 4 Powder infrared absorption spectrum of alumovesuvianite

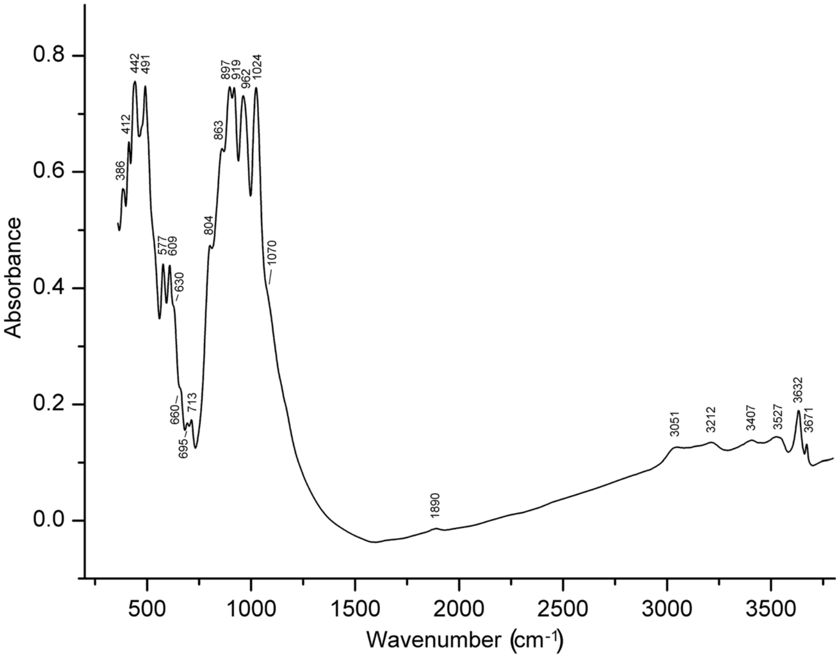

1983; Fitzgerald et al. 1986; Pavese et al. 1998; Armbruster and Gnos 2000a, c).

Vesuvianite usually contains significant amounts of Al_2O_3 ranging from 5.54 to 21.62 wt% (Groat et al. 1992; Fitzgerald et al. 1986), with Al^{3+} cations mostly in an octahedral coordination. The presence of five-coordinated Al in vesuvianites was reported by Phillips et al. (1987) and Olejniczak and Żabiński (1996) for Fe-poor vesuvianites from Asbestos, Luning, Georgetown (North America), and Piz Lunghin (Switzerland).

In this paper, we present data on alumovesuvianite (IMA 2016–014), ideally $Ca_{19}Al(Al,Mg)_{12}Si_{18}O_{69}(OH)_9$, a new vesuvianite-group mineral with Al as a dominant cation at the at the combined *Y*1 site. Both the new mineral and its name have been approved by the IMA CNMNC. The type specimens are deposited in the systematic collection of the Fersman Mineralogical Museum of the Russian Academy of Sciences, Moscow, Russia, under the registration numbers 4829/1 (holotype) and 4829/2 (cotype).

Characterization of alumovesuvianite

Occurrence

The type material of alumovesuvianite was collected in the abandoned Jeffrey mine, Asbestos, Estrie Region, Québec, Canada. For a long time this mine had been famous for gem-quality pink, purple and green vesuvianite crystals (Amabili et al. 2004). Alumovesuvianite occurs in the rodingite zone at

Table 1 Chemical composition of alumovesuvianite

Oxide*	Mean (wt%)	Range (wt%)	SD** (wt%)	Calibrant	Crystal	Characteristic Line
SiO_2	37.08	36.22–37.68	0.20	SiO_2	PET	Si *Kα*
Al_2O_3	18.82	18.72–19.29	0.19	Al_2O_3	TAP	Al *Kα*
CaO	36.57	34.99–37.07	0.27	$CaSO_4$	PET	Ca *Kα*
MgO	2.48	1.60–2.84	0.09	MgO	TAP	Mg *Kα*
Mn_2O_3***	0.67	0.37–0.86	0.05	Mn	LiF	Mn *Kα*
Fe_2O_3***	0.22	0.00–0.80	0.04	Fe_2O_3	LiF	Fe *Kα*
H_2O	2.61					
Total	98.45					

*Silicon, Al, Ca, Mg, Mn and Fe were measured by SEM–WDS, and H_2O was measured by TGA

***SD* standard deviation

*** The chemical formula for alumovesuvianite was calculated on the basis of trivalent Mn and Fe for stoichiometry reasons. Vesuvianite-group minerals usually has an average charge of the Y cations of 2.85^+ (Armbruster et al. 2002). Purplish pink color of the mineral indicates the presence of Mn^{3+}

the contact of a gabbroid rock with host serpentinite and definitely has a low-temperature (< 350 °C) hydrothermal origin (Wares and Martin 1980). The main minerals of the rodingite are diopside, grossular, alumovesuvianite and prehnite.

General appearance, physical properties and optical data

Alumovesuvianite forms prismatic crystals up to 4 × 4 × 6 mm^3 in size encrusting walls of cavities in granular diopside (Fig. 1). Individual crystals up to 6 mm long are elongated parallel to [001] and have the {100}, {110} and/or {210} prismatic forms and striation along [001]. The crystals are terminated by the {111}, {101}, {001} forms and sometimes by the {112} and/or {221} pyramids. Alumovesuvianite crystals are transparent colorless to purplish pink with a vitreous lustre. Cleavage is not observed; Mohs' hardness is 6.5. Density measured by flotation in diluted Clerici solution is 3.31(1) g/cm^3; density calculated using the empirical formula is 3.36 g/cm^3. The mineral is optically uniaxial (−), ω = 1.725(2), ε = 1.722(2) (in white light). Under microscope alumovesuvianite is colourless, nonpleochroic.

TGA and DSC analysis

Thermogravimetric (TG) measurements and differential scanning calorimetry (DSC) study were performed by

Table 2 X-ray powder diffraction data for alumovesuvianite

I_meas	d_meas (Å)	I_calc	d_calc (Å)	*hkl*	I_meas	d_meas (Å)	I_calc	d_calc (Å)	*hkl*
12	11.07	7	11.00	110	5	2.073	5	2.070	623
5	5.98	8	6.00	211	3	2.065	3	2.063	543
3	5.52	4	5.50	220	2	2.043	3	2.043	712
1	5.23	1	5.22	112	5	2.029	5	2.028	730
6	4.71	7	4.71	202	4	2.015	4	2.013	642
10	4.05	11	4.05	231	5	2.000	5	2.000	731
3	3.903	3	3.890	400	12	1.9632	11	1.9647	363
1	3.795	1	3.785	312	6	1.9279	4	1.9315	651
1	3.680	1	3.668	330	5	1.9219	3	1.9223	372
18	3.488	11	3.488	322	6	1.9062	3	1.9049	713
4	3.260	6	3.252	402	15	1.8882	11	1.8883	811
5	3.082	7	3.080	313	1	1.8729	2	1.8715	652
6	3.058	12	3.052	510	3	1.8001	1	1.8001	515
16	3.016	13	3.010	431	20	**1.7658**	12	1.7664	831
22	**2.969**	40	2.962	004	14	1.7178	6	1.7184	714
6	2.912	3	2.913	323	10	1.6813	7	1.6818	910
100	**2.761**	100	2.755	432	20	**1.6672**	18	1.6672	734
16	2.662	8	2.669	530	7	1.6479	3	1.6503	436
61	**2.612**	36	2.607	224	21	**1.6247**	19	1.6247	912
25	**2.593**	42	2.593	600	7	1.5870	3	1.5870	931
5	2.539	4	2.538	314	9	1.5718	6	1.5718	725
15	2.459	30	2.460	620	6	1.5573	14	1.5591	770
5	2.384	5	2.381	541	1	1.5435	1	1.5437	664
8	2.354	6	2.356	404	2	1.5381	4	1.5399	754
14	2.334	9	2.332	523	2	1.5251	2	1.5258	626
4	2.308	4	2.304	334	2	1.5115	3	1.5114	1020
3	2.279	3	2.276	631	4	1.5030	5	1.5050	950
1	2.245	2	2.243	215	4	1.4853	2	1.4863	1002
9	2.201	8	2.201	170	1	1.4540	1	1.4547	914
2	2.186	3	2.185	701	2	1.4460	2	1.4454	228
7	2.165	5	2.164	711	3	1.4221	1	1.4239	1032
3	2.146	2	2.145	504	4	1.3882	7	1.3884	308
8	2.138	9	2.135	315	5	1.3750	6	1.3754	774
2	2.090	5	2.088	432	22	**1.3443**	14	1.3437	880

The most intense lines ($I \geq 20\%$ of the intensity of the 2.761 Å line) are marked bold means of a NETZSCH STA 449 F3 Jupiter thermoanalyzer, in a dynamic argon atmosphere (with aluminum oxide standard, at heating rate of 10 °C/min, sample mass of 81.3 mg and temperature range from room temperature to 1100 °C).

The TGA and DSC curves (Fig. 2) of alumovesuvianite correspond to a low-symmetry vesuvianite which usually has a one-step weight loss with a sharp endothermic peak in the temperature range of 820–1090 °C (Żabinski et al. 1996). Endothermic effect at 1035 °C can be assigned to the dehydroxylation process (Foldvari 2011). Total weight loss for alumovesuvianite is 2.61%, which is in good agreement with the calculated H_2O content of 2.82%.

^{27}Al MAS NMR study

The ^{27}Al NMR (nuclear magnetic resonance) spectrum was obtained at room temperature by means of a Bruker Avance III 400 WB spectrometer at 104.24 MHz. The MAS (magic-angle spinning) spin rate of the rotor was 20 kHz. For these investigations, a single-pulse sequence with a pulse length of 86 kHz was used, with the recycle delay 1 s and the number of scans 4096.

The NMR spectrum (Fig. 3) of alumovesuvianite contains two peaks centered at −7.96 and 39.15 ppm. The group of overlapping peaks centered at −7.96 ppm are assigned to an octahedrally coordinated Al at the *Y*2(A,B) and *Y*3(A,B) sites (Phillips et al. 1987). According to Phillips et al. (1987) and Olejniczak and Żabiński (1996), the weak peak at 39.41 ppm has been assigned to Al at the 5-coordinated *Y*1A,B sites. Integral intensities of the peaks of $^{[6]}$Al and $^{[5]}$Al in the ^{27}Al NMR spectrum of holotype alumovesuvianite relate as 91.8% to 8.2%. The weak symmetric peaks observed at ±125 ppm belong to spinning sidebands; their positions differ from values of ±60 ppm reported by Phillips et al. (1987) due to the different spin rates.

Infrared spectroscopy

A powdered sample of alumovesuvianite was mixed with KBr, pelletized, and analyzed using an ALPHA FTIR spectrometer (Bruker Optics) at the resolution of 4 cm^{-1} and the total of 16 scans in the range between 360 and 3800 cm^{-1}. The

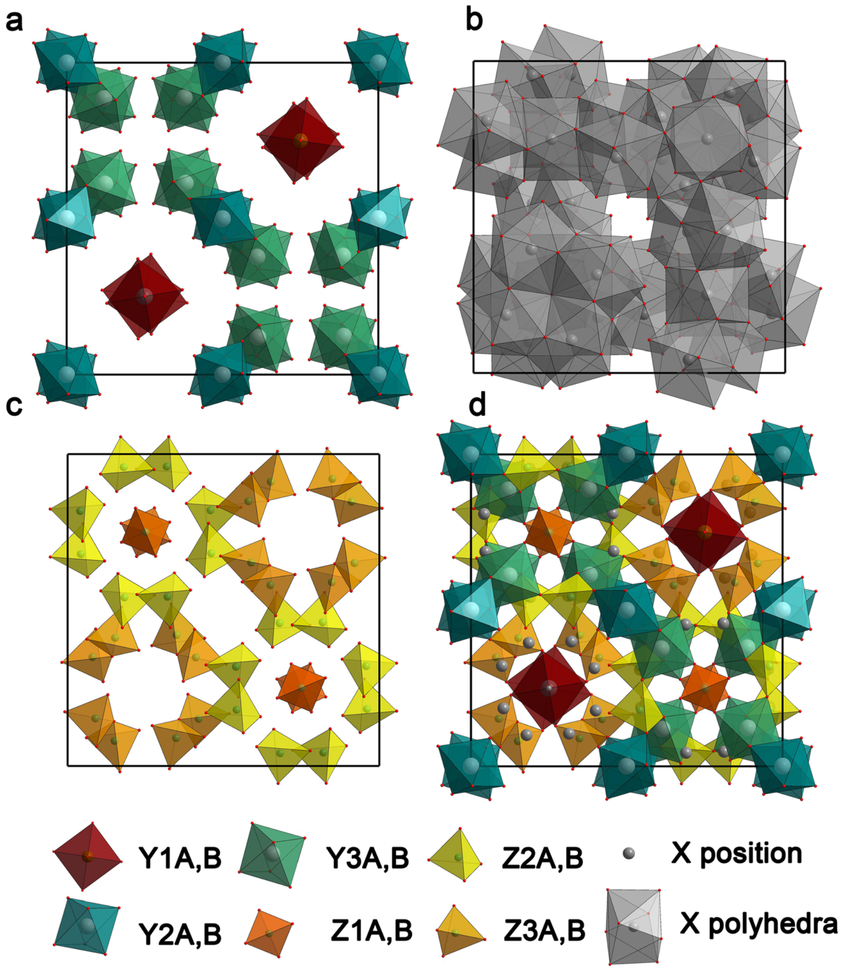

Fig. 5 Projections of alumovesuvianite structure along the *c* axis. **a** arrangement of *Y*-cation polyhedra: *dark green* and *light green* octahedra represent of *Y*2A,B and *Y*3A,B positions; red square pyramid represent *Y*1A,B sites, occupied by Al **b** arrangement of *X*-cation polyhedra: grey polyhedra, grey spheres represent polyhedra and atoms of Ca **c** arrangement of *Z*-cation polyhedra: bright orange, orange, yellow represent *Z*1A,B; *Z*2A,B and *Z*3A,B tetrahedra, respectively; **d** common arrangement of the alumovesuvianite crystal structure

IR spectrum of an analogous pellet of pure KBr was used as a reference.

The IR spectrum of alumovesuvianite (Fig. 4) contains bands of O–H-stretching vibrations (in the range from 3000 to 3700 cm^{-1}), strong bands of Si–O-stretching vibrations (in the range from 860 to 1070 cm^{-1}), as well as Si–O–Si and O–Si–O bending vibrations, partly combined with stretching vibrations of *Y*-centered polyhedra (below 630 cm^{-1}). The bands in the range from 690 to 810 cm^{-1} are assigned to bending vibrations of OH^- groups. The absence of absorption bands in the range 1100–1500 cm^{-1} indicates the absence of boron-bearing groups. The weak band at 1890 cm^{-1} corresponds to overtone or combination mode of Si–O-stretching vibrations.

The bands of O–H-stretching vibrations at 3671, 3632, 3527, 3407, 3212 and 3051 cm^{-1} correspond to the A, B, E, G, J, and M bands, respectively, which are predominantly polarized along *c* and correspond to differently coordinated OH groups at the O11 (the bands A, B, E, and G) and O10 (the bands J and M) sites (Groat et al. 1995).

Chemical data

Chemical analyses (Table 1) were obtained using a HITACHI S-3400 N SEM (scanning electron microscope) equipped with INCA Wave 500 WDS (wavelength-dispersive spectroscopy) spectrometer. The system was operated at 20 kV and 10 nA, and the electron beam was focused to a 5 μm spot. Contents of elements (other than those reported in Table 1) having atomic numbers higher than eight are below the detection limits. The H_2O content was analyzed by thermogravimetric analysis (TGA). The empirical formula of alumovesuvianite, calculated on the basis of 19 Ca apfu and taking into account the MAS NMR data, is: $Ca_{19.00}(Al_{0.92}Fe^{3+}_{0.08})_{\Sigma 1.00}(Al_{9.83}Mg_{1.80}Mn^{3+}_{0.25})_{\Sigma 11.88}Si_{17.98}O_{69.16}(OH)_{8.44}$. The idealized formula of the Al-dominant end-member is $Ca_{19}Al(Al_{10}Mg_2)Si_{18}O_{69}(OH)_9$, which requires MgO 2.82 wt%, CaO 37.1 wt%, Al_2O_3 19.5 wt%, SiO_2 37.7 wt%, and H_2O 2.82 wt%. The Gladstone-Dale compatibility index (Mandarino 1981) is −0.016 (superior) if D_{calc} is used and −0.029 (excellent) if D_{meas} is used.

X-ray crystallography

Powder X-ray diffraction data (Table 2) were collected by means of a Bruker Phazer D2 diffractometer in the 2θ range of 5–70° (CuKα; 1.5418 Å) with scanning steps of 0.02° (1 s per step) in 2θ. The unit-cell dimensions determined from the corrected X-ray powder-diffraction by Rietveld refinement using the program Topas 4.2 (Bruker 2009) are as follows: $a = 15.5603(5)$ Å, $c = 11.8467(4)$ Å, $V = 2868.3(4)$ $Å^3$.

The single-crystal X-ray diffraction experiment was carried out using an Agilent Technologies Xcalibur Eos diffractometer operated at 50 kV and 40 mA. A hemisphere of three-dimensional data was collected at 100 K using monochromatic MoK_α X-radiation with frame widths of 1° and 80 s count for each frame. Crystal-to-detector distance was 45 mm. For the investigated sample 624 systematic absence violations with $I > 3\sigma(I)$ have been observed, of which 616 ones correspond to $0kl$ with $k + l \neq 2n$, hkl with $h = k$ and $l \neq 2n$ (see Armbruster and Gnos 2000b) and therefore consistent with the space group *P*4/*n*. The strongest reflections of this type are 003, 005, 007, 0011, 014, 016, 018 with $10\sigma(I) < I < 50\sigma(I)$. Only 8 observed violations with the $3\sigma(I) < I < 8\sigma(I)$ are the $hk0$ reflections with $h + k \neq 2n$ in agreement with the presence domains with the *P*4*nc* symmetry. In accordance with the observed systematic absences the *P*4/*n* space group was chosen for structural refinement.

The crystal structure of alumovesuvianite (Fig. 5) was refined to $R_1 = 0.036$ for 3098 unique observed reflections with $|F_o| \geq 4\sigma_F$ by means of the *SHELX* program (Sheldrick 2008). Empirical absorption correction was applied in the CrysAlisPro (Agilent Technologies 2014) program complex using spherical harmonics, implemented in the SCALE3 ABSPACK scaling algorithm. Volumes of coordination polyhedra were calculated using the VESTA 3 program (Momma and Izumi 2011). Hydrogen atoms of the OH^- groups were localized from the difference Fourier maps and added to the refinement model. Since the restraint-free refinement

Table 3 Single-crystal data and structure refinement for alumovesuvianite

Temperature (K)	100(2)
Crystal system	tetragonal
Space group	*P*4/*n*
$a = b$ (Å)	15.51033(19)
c (Å)	11.8096(2)
α (°) = β (°) = γ (°)	90
Cell volume ($Å^3$)	2841.05(9)
Z	2
ρ_{calc} (g/cm^3)	3.370
μ (mm^{-1})	2.563
F (000)	2875.0
Crystal size (mm^3)	0.21 × 0.17 × 0.14
Radiation / wavelength (Å)	MoKα / 0.71073
2θ range for data collection (°)	5.3–55.0
Index ranges	$-20 \leq h \leq 20$; $-15 \leq k \leq 19$; $-15 \leq l \leq 15$
Reflections collected	12,750
Independent reflections	3265 [$R_{int} = 0.0249$, $R_{sigma} = 0.0224$]
Number of restraints / parameters	3 / 309
Goodness-of-fit on F^2	1.323
Final *R* indexes [I > =2σ (I)]	$R_1 = 0.0363$, $wR_2 = 0.0809$
Final *R* indexes [all data]	$R_1 = 0.0386$, $wR_2 = 0.0816$
Largest difference peak / hole ($e^- Å^{-3}$)	0.66 / -1.25

produced for the O11A,B-H bonds unacceptable shift/esd ratio > 0.01, hydrogen atoms were refined with the imposed O-H distance restraints of 1.00 Å. The final difference Fourier map showed no features higher than 0.66 e^- $Å^{-3}$. Experimental details and crystallographic parameters are given in Table 3. The final atomic coordinates and isotropic

Table 4 Atomic coordinates, displacement parameters and site-scattering factors for the alumovesuvianite structure

Site	Occupancy per site	Occupancy per formula unit (apfu)	*x*	*y*	*z*	U_{eq} ($Å^2$)	*s.s.f.* (e^-)
*Z*1A	1	Si	1/4	3/4	0	0.0057(4)	14
*Z*1B	1	Si	3/4	1/4	1/2	0.0051(4)	14
*Z*2A	1	4 Si	0.67964(6)	0.45785(6)	0.12717(8)	0.00414(19)	14
*Z*2B	1	4 Si	0.46007(6)	0.68203(6)	0.36915(8)	0.00419(19)	14
*Z*3A	1	4 Si	0.34938(6)	0.42027(6)	0.13655(8)	0.0043(2)	14
*Z*3B	1	4 Si	0.41117(6)	0.34803(6)	0.36691(8)	0.0050(2)	14
*X*1	1	2 Ca	3/4	1/4	0.24990(8)	0.0046(2)	20
*X*2A	1	4 Ca	0.54225(4)	0.30981(4)	0.12159(6)	0.00453(15)	20
*X*2B	1	4 Ca	0.31188(4)	0.54586(4)	0.38088(6)	0.00477(15)	20
*X*3A	1	4 Ca	0.60407(5)	0.68557(5)	0.10418(6)	0.00729(16)	20
*X*3B	1	4 Ca	0.67828(5)	0.59957(5)	0.37759(6)	0.00806(16)	20
*X*4A	0.07(1)	0.07 Ca	1/4	1/4	0.3493(17)	0.0062(3)	1.46
*X*4B	0.93(1)	0.93 Ca	1/4	1/4	0.15023(13)	0.0062(3)	18.54
*Y*2A	1	2Al	1/2	1/2	0	0.0038(3)	13.00
*Y*2B	1	2Al	1/2	1/2	1/2	0.0049(3)	13.00
*Y*3A	1	3.60 Al + 0.40 Mg	0.38897(7)	0.62265(7)	0.12661(9)	0.0045(2)	13.00
*Y*3B	1	2.40 Al + 1.60 Mg	0.61928(7)	0.38642(7)	0.37467(9)	0.0062(2)	13.00
*Y*1A	0.93(1)	0.73 Al + 0.20 Mn	1/4	1/4	0.52998(17)	0.0061(6)	14.49
*Y*1B	0.07(1)	0.07 Fe	1/4	1/4	0.0392(13)	0.0061(6)	1.82
O1A	1	4 O	0.28235(16)	0.67278(16)	0.0856(2)	0.0052(5)	8
O1B	1	4 O	0.67189(16)	0.27863(16)	0.4144(2)	0.0060(5)	8
O2A	1	4 O	0.65748(16)	0.38149(16)	0.2194(2)	0.0063(5)	8
O2B	1	4 O	0.38316(16)	0.66151(16)	0.2766(2)	0.0054(5)	8
O3A	1	4 O	0.45044(15)	0.72259(16)	0.0754(2)	0.0046(5)	8
O3B	1	4 O	0.72111(16)	0.45215(16)	0.4236(2)	0.0059(5)	8
O4A	1	4 O	0.60579(15)	0.43623(16)	0.0269(2)	0.0053(5)	8
O4B	1	4 O	0.43894(16)	0.60696(16)	0.4675(2)	0.0066(5)	8
O5A	1	4 O	0.33226(16)	0.51859(16)	0.1800(2)	0.0067(5)	8
O5B	1	4 O	0.50913(17)	0.32674(16)	0.3240(2)	0.0082(5)	8
O6A	1	4 O	0.27047(16)	0.38608(17)	0.0620(2)	0.0079(5)	8
O6B	1	4 O	0.37121(18)	0.27168(16)	0.4436(2)	0.0106(5)	8
O7A	1	4 O	0.67021(16)	0.55562(16)	0.1737(2)	0.0064(5)	8
O7B	1	4 O	0.55609(16)	0.67557(16)	0.3166(2)	0.0078(5)	8
O8A	1	4 O	0.43956(16)	0.41000(16)	0.0687(2)	0.0063(5)	8
O8B	1	4 O	0.40697(16)	0.43836(16)	0.4370(2)	0.0055(5)	8
O9	1	4 O	0.35166(16)	0.35762(16)	0.2507(2)	0.0069(5)	8
O10A	1	O	3/4	3/4	0.3741(4)	0.0101(11)	8
O10B	1	O	3/4	3/4	0.1423(4)	0.0066(10)	8
O11A	1	4O	0.49569(16)	0.56346(17)	0.1349(2)	0.0063(5)	8
O11B	1	4O	0.55924(17)	0.49466(16)	0.3629(2)	0.0077(5)	8
H10B	1	H	3/4	3/4	0.2275(18)	0.02(3)	
H11B	1	4H	0.524(5)	0.495(5)	0.293(4)	0.09(3)	
H11A	1	4H	0.549(4)	0.563(6)	0.182(7)	0.11(3)	

The refined formula is $Ca_{19}(Al_{0.73}Mn_{0.20}Fe_{0.07})_{1.00}(Al_{10.00}Mg_{2.00})_{12}(SiO_4)_{10}(Si_2O_7)_4[(OH)_9O]_{10}$

displacement parameters are in Table 4. Selected interatomic distances, anisotropic displacement parameters and information on polyhedral volumes of cations can be obtained from the electronic supplementary materials (Tables S 1–3). The geometry of the hydrogen bonding system (Table 5) is typical for F-free vesuvianites (Pavese et al. 1998; Lager et al. 1999).

Both mean < Z–O > bond lengths and scattering factors of tetrahedral *Z*1A,B; *Z*2A,B and *Z*3A,B sites are in agreement with full occupancies of this sites by Si atoms only. There are no evidences of the SiO_4^{4-}↔$[H_4O_4]^{4-}$ substitution (Galuskin et al. 2007).

In the crystal structure of alumovesuvianite, the 7–9 coordinated *X*1, *X*2A,B, *X*3A,B and *X*4A,B sites are fully populated by Ca atoms. The *X* sites have full occupancies except for the eightfold-coordinated *X*4A and *X*4B positions, which are situated in the structure channels and have populations of 0.07 and 0.93, respectively.

The key specific feature that defines alumovesuvianite as a new mineral species is the population of the *Y*1A,B sites that have a square-pyramidal coordination. In the vesuvianite-group minerals, these sites can be predominantly occupied by Cu^{2+}, $Fe^{2+,3+}$, Mn^{3+}, Mg and Al (Phillips et al. 1987; Olejniczak and Żabiński 1996; Ohkawa et al. 1992; Armbruster et al. 2002; Panikorovskii et al. 2016b). The crystal-structure studies by Fitzgerald et al. (1986) indicated that, in Fe-free (Al-rich) vesuvianites from Asbestos, Quebec, Canada, Al is incorporated into the *Y*1A,B sites. In alumovesuvianite, Al prevails in the (*Y*1A,B) sites (Fig. 6). The average < *Y*1A − O > and <*Y*1B − O > bond lengths are 1.916 (occupation by 0.93 apfu with predominant Al) and 2.150 (occupation by 0.07 Fe apfu) Å, respectively, where the distance of 1.916 Å is in a rather good agreement (taking into account 0.93 occupancy factor) with the <Al − O > bond length of 1.87 Å for a five-coordinated Al^{3+} according to Shannon (1976). The *s.s.f.* (site-scattering factors; in e^-) value for the sum of *Y*1A,B sites is 16.31 epfu (electrons per formula unit), which is in accordance with the MAS-NMR data indicating that the pair of *Y*1 sites is predominantly occupied by Al. Considering the MAS-NMR data, the total occupation pair of the *Y*1 sites requires $(Al_{0.73}Mn_{0.20}{}^{3+}Fe_{0.07}{}^{3+})_{\Sigma 1.00}$. The *Y*2A and *Y*2B sites are fully occupied by Al, in agreement with the average < *Y*2A − O > and <*Y*2A − O > bond lengths of 1.894 and 1.898 Å, respectively. The average < *Y*3A − O > and <*Y*3B − O > bond lengths are 1.925 and 1.974 Å, and the calculated occupancies of the *Y*3A and *Y*3B sites are $(Al_{0.90}Mg_{0.10})_{\Sigma 1.00}$ and $(Al_{0.60}Mg_{0.40})_{\Sigma 1.00}$, respectively.

Table 5 Selected interatomic distances, angles and distances between nearest anions for hydrogen bonds in structure of alumovesuvianite

D–H (Å)	H···A (Å)	D···A (Å)	D–H–A (°)	Hydrogen bond
1.01(2)	1.73(2)	2.737(7)	180.000(2)	O10B–H10B... O10A
0.99(2)	1.89(6)	2.748(4)	142(7)	O11A–H11A... O7A
0.99(2)	2.19(5)	3.059(3)	145(7)	O11B–H11B... O11A

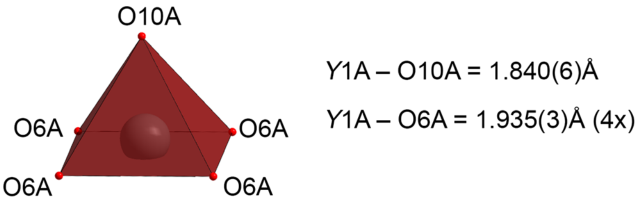

Fig. 6 Square-pyramidal coordination of Al and distances between *Y*1 site and O atoms

The total crystal-chemical formula of alumovesuvianite derived on the basis of crystal-structure refinement and taking account the MAS NMR data can be written as follows: $(Ca)^{X1}{}_{2.00}(Ca)^{X2A}{}_{4.00}(Ca)^{X2B}{}_{4.00}(Ca)^{X3A}{}_{4.00}(Ca)^{X3B}{}_{4.00}(Ca)^{X4A}{}_{0.07}(Ca)^{X4B}{}_{0.93}(Al_{0.73}Mn_{0.20})^{Y1A}{}_{\Sigma 0.93}(Fe)^{Y1B}{}_{0.07}(Al)^{Y2A}{}_{2.00}(Al)^{Y2B}{}_{2.00}(Al_{3.60}Mg_{0.40})$

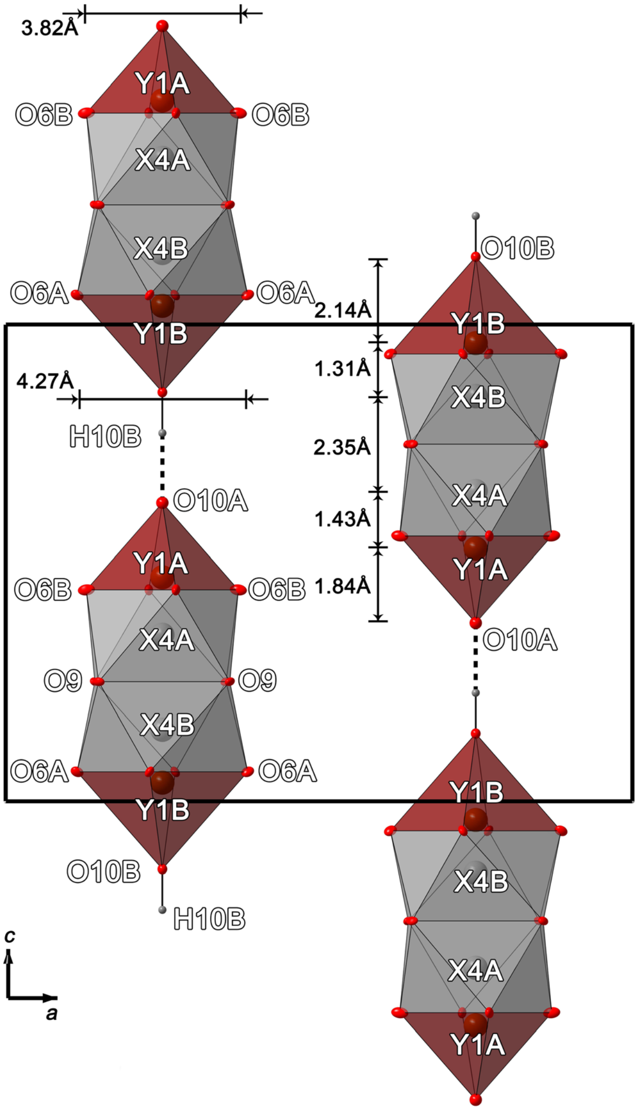

Fig. 7 Configuration of the cation strings ('rods') in the alumovesuvianite structure

$^{Y3A}{}_{\Sigma 4.00}(Al_{2.40}Mg_{1.60})^{Y3B}{}_{\Sigma 4.00}(Si)^{Z1A}{}_{1.00}(Si)^{Z1B}{}_{1.00}(Si)^{Z2\text{-}A}{}_{4.00}(Si)^{Z2B}{}_{4.00}(Si)\ ^{Z3A}{}_{4.00}(Si)^{Z3B}{}_{4.00}O_{68.00}(OH_{9.00}O)_{\Sigma 10.00}$. The simplified formula obtained from the structure refinement is: $Ca_{19}(Al_{0.73}Mn^{3+}{}_{0.20}Fe^{3+}{}_{0.07})_{1.00}(Al_{10.00}Mg_{2.00})_{12.00}Si_{18}O_{69}(OH)_9$.

Discussion

It has been known that different vesuvianite samples from the Jeffry mine have different amounts of Fe_2O_3 (Groat et al. 1992; Lafuente et al. 2015 - RRUF id R050056 and R060170). Vesuvianites with the substantial content of Fe_2O_3 (1.42 wt% according to Groat et al. 1992) occur as often as varieties with low amounts of Fe_2O_3 (0.05–0.29 wt%, Fitzgerald et al. 1986; Phillips et al. 1987). Structural investigation of the Fe-free sample with the *P*4/*n* symmetry showed the dominant role of Al at the *Y*1A,B sites (Fitzgerald et al. 1986). Investigations by the ^{27}Al MAS NMR by Phillips et al. (1987) indicated 0.8 apfu of five-coordinated Al and confirmed the conclusion of Fitzgerald et al. (1986), which agrees very well with our data presented herein.

In the crystal structure of vesuvianite, the *Y*1A,B sites are usually occupied by Fe^{3+} (Giuseppetti and Mazzi 1983; Panikorovskii et al. 2016b). According to Panikorovskii et al. (2016d), the absence of significant amounts of Fe in the mineral is the most plausible explanation for the occurrence of magnesiovesuvianite (i.e. the incorporation of Mg into *Y*1 sites). The same precondition can also be assigned to alumovesuvianite. The Al/Mg ratio in the *Y*1 sites in these two minerals depends upon the degree of cation ordering in structural rods and, consequently, upon thermodynamic conditions of the mineral formation. In vesuvianite samples with a high degree of order (Armbruster and Gnos 2000c), such as alumovesuvianite, an unequal distribution of Mg between *Y*3A and *Y*3B sites has been observed.

In the FTIR spectra there are two evident bands 3051(M) and 3212 (J) related to the two configurations of the OH groups in the structure channels. According to Groat et al. (1995), the J band should be attributed to the OH–Fe^{2+} configuration, which is not presented in our sample. Most likely, these two bands correspond to the Al–OH and Fe^{3+}–OH configurations that involve the H10B site.

According to the model of structure relaxation proposed by Panikorovskii et al. (2016d) for cyprine, ordering in the pairs of the *X*4A-*X*4B and *Y*1B-*Y*1A sites affects the distribution of Mn and Mg between the octahedral *Y*3A,B sites. In the case of alumovesuvianite, significant increase of the O6A − O6A distance (i.e. the diagonal of the base square antiprism) up to 4.27 Å (Fig. 7) due to practically full occupancy of the *X*4B site ($Ca_{0.93}$ with the respective polyhedral volume of 24.74 Å^3) results in the relative compression of the *Y*3A octahedra in the same polyhedral sheet (occupancy $Al_{0.90}Mg_{0.10}$, $V = 9.41$ Å^3 and the average < *Y*3A − O > bond length of 1.925 Å). The respective compression of the *X*4A polyhedra (O6B − O6B = 3.82 Å, occupancy $Ca_{0.07}$ and $V = 22.68$ Å) is compensated by the expansion of the *Y*3B polyhedra (occupancy $Al_{0.60}Mg_{0.40}$ and $V = 10.16$ Å^3, average < *Y*3B − O > bond lengths of 1.974 Å).

Consequently, some Fe-poor (<0.5 *pfu*) disordered vesuvianite species (with the *P*4/*nnc* symmetry) such as Norwegian “cyprines” from Sauland (Panikorovskii et al. 2016a) do not have unequal distribution of Mg between octahedral sites and should probably be considered as magnesiovesuvianite or cyprine depending upon the dominant cation in the *Y*1 site. On the other hand, highly ordered vesuvianite-group mineral from Georgetown, USA (Phillips et al. 1987) should now be considered as alumovesuvianite.

Acknowledgements The authors are grateful to Gregory Yu. Ivanyuk for the photograph of the alumovesuvianite specimen. Fernando Cámara, Evgeny V. Galuskin and editor Lutz Nasdala are thanked for critical reviews and helpful comments. This work was supported by St. Petersburg State University (3.38.243.2015) and the President of Russian Federation Grant for leading scientific schools (no. NSh-10005.2016.5). Experimental studies were carried out using resources of the X-ray Diffraction Centre and Geo Environmental Centre “Geomodel” of Saint-Petersburg State University.

References

Agilent Technologies (2014) CrysAlis CCD and CrysAlis RED. Oxford Diffraction Ltd, Yarnton, Oxfordshire, UK

Aksenov SM, Chukanov NV, Rusakov VS, Panikorovskii TL, Gainov RR, Vagizov FG, Rastsvetaeva RK, Lyssenko KA, Belakovskiy DI (2016) Towards a revisitation of vesuvianite-group nomenclature: the crystal structure of Ti-rich vesuvianite from Alchuri, Shigar valley, Pakistan. Acta Crystallogr B72:744–752

Allen FM, Burnham CW (1992) A comprehensive structure-model for vesuvianite: symmetry variations and crystal growth. Can Mineral 30:1–18

Amabili M, Miglioli A, Spertimi F (2004) Recent discoveries at the Jeffrey mine asbestos, Québec. Mineral Rec 35(2):123–135

Armbruster T, Gnos E (2000a) *P*4/*n* and *P*4*nc* long range ordering in low-temperature vesuvianites. Am Mineral 85:563–569

Armbruster T, Gnos E (2000b) Tetrahedral vacancies and cation ordering in low-temperature Mn-bearing vesuvianites: indication of hydrogarnet-like substitution. Am Mineral 85:570–577

Armbruster T, Gnos E (2000c) “rod” polytypism in vesuvianite: crystal structure of a low-temperature *P*4*nc* with pronounced octahedral cation ordering. Schweiz Miner Petrog 80:109–116

Armbruster T, Gnos E, Dixon R, Gutzmer J, Hejny C, Döbelin N, Medenbach O (2002) Manganvesuvianite and tweddillite, two new Mn^{3+}-silicate minerals from the Kalahari manganese fields, South Africa. Mineral Mag 66:137–150

Bruker AXS (2009) Topas V4.2: General profile and structure analysis software for powder diffraction data. Karlsruhe, Germany.

Coda A, Giusta DA, Isetti G, Mazzi F (1970) On the structure of vesuvianite. At D Ac Del Sci di Torino 105:1–22

Dyrek K, Platonov AN, Sojka Z, Żabinski W (1992) Optical absorption and EPR study of Cu^{2+} ions in vesuvianite ("cyprine") from Sauland, Telemark, Norway. Eur J Mineral 4:1285–1289

Fitzgerald S, Rheingold AL, Leavens PB (1986) Crystal structure of a non-*P*4/*nnc* vesuvianite from asbestos, Quebec. Am Mineral 71: 1483–1488

Foldvari M (2011) Handbook of thermogravimetric system of minerals and its use in geological practice. Geological Institute of Hungary ed, Budapest, 180 pp

Galuskin EV, Galuskina IO, Sitarz M, Stadnicka K (2003) Si-deficient, OH-substituted, boron-bearing vesuvianite from the Wiluy River, Yakutia, Russia. Can Mineral 41:833–842

Galuskin EV, Galuskina IO, Dzierzanowski P (2005) Chlorine in vesuvianites. Mineral Pol 36:51–61

Galuskin EV, Galuskina IO, Stadnicka K, Armbruster T, Kozanecki M (2007) The crystal structure of Si-deficient, OH-substituted, boron-bearing vesuvianite from the Wiluy River, Sakha-Yakutia. Russia; Can Mineral 45:239–248

Giuseppetti G, Mazzi F (1983) The crystal structure of a vesuvianite with *P*4/*n* symmetry. Tscher Miner Petrog 31:277–288

Gnos E, Armbruster T (2006) Relationship among metamorphic grade, vesuvianite "rod polytypism", and vesuvianite composition. Am Mineral 91:862–870

Groat LA, Hawthorne FC, Ercit TS (1992) The chemistry of vesuvianite. Can Mineral 33:19–48

Groat LA, Hawthorne FC, Rossman GR, Scott TE (1995) The infrared spectroscopy of vesuvianite in the OH region. Can Mineral 33:609–626

Krivovichev SV (2013) Structural complexity of minerals: information storage and processing in the mineral world. Mineral Mag 77(3): 275–326

Lafuente B, Downs RT, Yang H, Stone N (2015) The power of databases: the RRUFF project. In: Armbruster T, Danisi RM (eds) Highlights in mineralogical crystallography. W De Gruyter, Berlin, Germany, pp 1–30

Lager GA, Xie Q, Ross FK, Rossman GR, Armbruster T, Rotella FJ, Schultz AJ (1999) Hydrogen-atom position in *P*4/*nnc* vesuvianite. Can Mineral 37:763–768

Machatschki F (1932) Zur Formel des Vesuvian. Z Kristallogr 81:148–152

Mandarino JA (1981) The Gladstone – dale relationship: part IV. The compatibility concept and its application. Can Mineral 19:441–450

Momma K, Izumi F (2011) VESTA 3 for three-dimensional visualization of crystal, volumetric and morphology data. J Appl Crystallogr 44: 1272–1276

Ohkawa M, Yoshiasa A, Takeno S (1992) Crystal chemistry of vesuvianite: site preferences of square-pyramidal coordinated sites. Amer Mineral 77:945–953

Olejniczak Z, Żabiński W (1996) ^{27}Al NMR study of white vesuvianite from Piz Lunghin, Switzerland. Mineral Pol 27:41–45

Panikorovskii TL, Zolotarev AA Jr, Krivovichev SV, Shilovskikh VV, Bazai AV (2016a) Crystal chemistry of Cu-bearing vesuvianites ("cyprine") from Kleppan (Norway). Zap Ross Mineral Obsh 145(1):131–142 (in Russian)

Panikorovskii TL, Krivovichev SV, Zolotarev AA Jr, Antonov AA (2016b) Crystal chemistry of low-symmetry (*P*4*nc*) vesuvianite from the Kharmankul' cordon (south Urals, Russia). Zap Ross Mineral Obsh 145(3):94–104 (in Russian)

Panikorovskii TL, Chukanov NV, Aksenov SM, Mazur AS, Avdontseva EY, Shilovskikh VV (2016c) Alumovesuvianite, IMA 2016-014. CNMNC newsletter no. 32, august 2016, page 916. Mineral Mag 80:915–922

Panikorovskii TL, Shilovskikh VV, Avdontseva EY, Zolotarev AA Jr, Pekov IV, Britvin SN, Hålenius U, Krivovichev SV (2016d) Cyprine, $Ca_{19}Cu^{2+}(Al,Mg)_{12}Si_{18}O_{69}(OH)_9$, a new vesuvianite-group mineral from the Wessels mine, South Africa Eur J Mineral (in press) DOI: 10.1127/ejm/2017/0029-2592

Panikorovskii TL, Shilovskikh VV, Avdontseva EY, Zolotarev AA Jr, Karpenko VY, Mazur AS, Yakovenchuk VN, Krivovichev SV, Pekov IV (2016e) Magnesiovesuvianite, $Ca_{19}Mg(Al,Mg)_{12}Si_{18}O_{69}(OH)_9$, a new vesuvianite-group mineral. J Geosc (in press).

Pavese A, Prencipe M, Tribaudino M, Aagaard SS (1998) X-ray and neutron single-crystal study of *P*4/*n* vesuvianite. Can Mineral 36: 1029–1037

Phillips BL, Allen FM, Kirkpatrick RJ (1987) High-resolution solid-state ^{27}Al NMR spectroscopy of Mg-rich vesuvianite. Am Mineral 72: 1190–1194

Shannon RD (1976) Revised effective ionic radii and systematic studies of interatomic distances in halides and chalcogenides. Acta Cryst A32:751–767

Sheldrick GM (2008) A short history of SHELX. Acta Crystallogr A64: 112–122

Wares RP, Martin RF (1980) Rodingitization of granite and serpentinite in the Jeffrey mine, asbestos Quebec. Can Mineral 18:231–240

Żabinski W, Wactawska Z, Paluszkiewicz C (1996) Thermal decomposition of vesuvianite. J Therm Anal 46:1437–1447